

Environmental Sustainability Assessment of Hydrogen from Waste Polymers

Cecilia Salah, Selene Cobo, Javier Pérez-Ramírez, and Gonzalo Guillén-Gosálbez*

Cite This: *ACS Sustainable Chem. Eng.* 2023, 11, 3238–3247

Read Online

ACCESS |

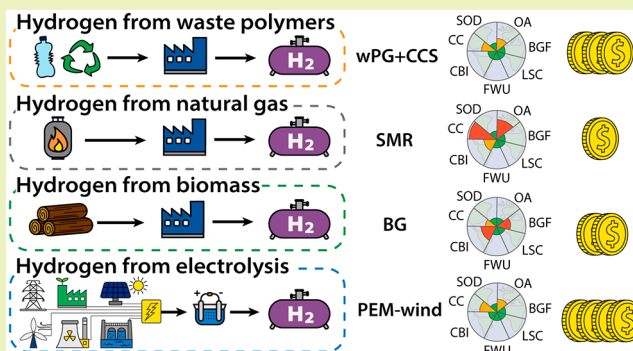
Metrics & More

Article Recommendations

Supporting Information

ABSTRACT: The rising demand for single-use polymers calls for alternative waste treatment pathways to ensure a circular economy. Here, we explore hydrogen production from waste polymer gasification (wPG) to reduce the environmental impacts of plastic incineration and landfilling while generating a valuable product. We assess the carbon footprint of 13 H₂ production routes and their environmental sustainability relative to the planetary boundaries (PBs) defined for seven Earth-system processes, covering H₂ from waste polymers (wP; polyethylene, polypropylene, and polystyrene), and a set of benchmark technologies including H₂ from natural gas, biomass, and water splitting. Our results show that wPG coupled with carbon capture and storage (CCS) could reduce the climate change impact of fossil-based and most electrolytic routes. Moreover, due to the high price of wP, wPG would be more expensive than its fossil- and biomass-based analogs but cheaper than the electrolytic routes. The absolute environmental sustainability assessment (AESAs) revealed that all pathways would transgress at least one downscaled PB, yet a portfolio was identified where the current global H₂ demand could be met without transgressing any of the studied PBs, which indicates that H₂ from plastics could play a role until chemical recycling technologies reach a sufficient maturity level.

KEYWORDS: Waste polymers gasification, Hydrogen, Life cycle assessment, Planetary boundaries, Techno-economic analysis



INTRODUCTION

The global demand for polymers is rising, leading to increasing amounts of waste polymers (wP). Only 9% of all plastics produced until 2015 were recycled, 12% incinerated, and the remaining 79% were landfilled or lost to the environment.¹ Moreover, within the plastic packaging sector (USD 80–120 billion annually),² 95% of polymers are single-use and have a short lifetime, with a low recycling rate of 14%.² In 2013, 72% of the 78 Mt of plastic packaging materials produced were landfilled or dispersed in the environment.² This waste mismanagement has detrimental consequences for ecosystems and human health,^{3–7} which underlines the need for a circular economy that valorizes wP.

Chemical recycling has recently gained attention for providing valuable feedstock that could replace fossil resources and help transition to a circular carbon economy,^{8–10} thereby avoiding the environmental impacts of incinerating and landfilling wP.^{11–13} For instance, waste polyethylene and polypropylene can undergo pyrolysis to recover their respective monomers^{14–17} or gasification to produce synthesis gas (a mixture of H₂, CO, and CO₂), widespread in chemical production.^{18,19} Although monomers should be the ultimate goal in chemical recycling, the gasification route appears easier

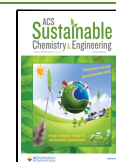
to implement, is more mature, and can handle mixed-polymer inlet streams.²⁰

Alternatively, gasification of wP could yield H₂ to decarbonize several sectors,²¹ including transportation and industry, responsible for 25.7% and 19.7% of all greenhouse gas (GHG) emissions in 2019, respectively.²² Steam methane reforming (SMR) is currently the preferred pathway to produce H₂ from natural gas (gray H₂), while blue H₂ from SMR coupled with carbon capture and storage (CCS) and green H₂ from electrolysis based on renewables or biomass gasification are still marginal. To date, SMR is the cheapest technology,²³ but other alternatives could reduce human health and ecosystems impacts substantially.²⁴ Notably, previous works applied life cycle assessment (LCA) to H₂ pathways, finding that gray H₂ embeds the highest global warming impacts (GWI) among existing technologies.²⁵ Moreover, Verma et al. showed that coupling CCS with SMR significantly reduces fossil-based H₂'s

Received: September 24, 2022

Revised: January 23, 2023

Published: February 13, 2023



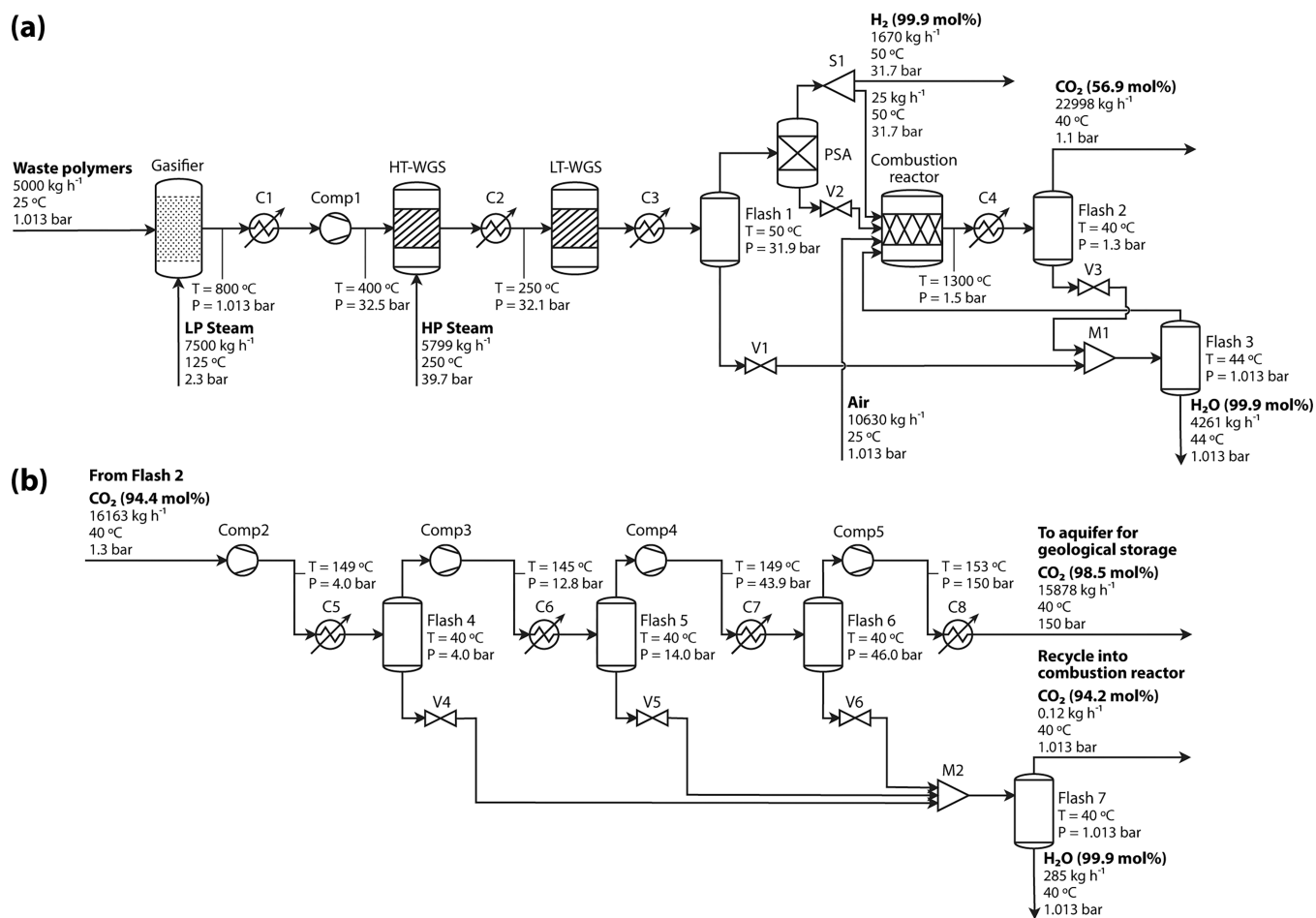


Figure 1. Process flowsheet of H₂ from waste polymers. (a) Waste polymer gasification (wPG). (b) CO₂ compression unit for CO₂ geological storage. Additional unit for the wPG process coupled with carbon capture and storage (wPG+CCS).

net life cycle GHG emissions (to less than half), making blue H₂ environmentally competitive against electrolytic H₂ from renewables.²⁵ Moreover, Bhandari et al. found that the electricity source heavily influences the environmental performance of electrolytic routes at the mid- and end point impact levels.²⁶ On the economic side, Lan and Yao recently discussed that producing H₂ via wP gasification in the US could yield competitive costs with blue H₂ in the local market.²⁷

LCA has become the preferred approach for evaluating the environmental impact of technologies.²⁸ However, standard LCAs are mostly applied to compare alternatives as they lack thresholds beyond which a system should be deemed unsustainable, making the interpretation phase challenging.²⁹ Absolute environmental sustainability assessment (AESA) studies have recently emerged to define environmental limits on impact metrics.^{30–32} Following this approach, the estimated environmental impacts of an anthropogenic system are evaluated against the maximum impact levels that could potentially shift the current state of the planet.³³ These limits can be derived from the planetary boundaries (PBs) framework, introduced by Rockström et al.³⁴ and later updated by Steffen et al.,³⁵ which represent ecological limits on nine Earth-system processes delimiting a safe operating space (SOS) for humanity. A recent study by Valente et al.³⁶ employed the AESA method to showcase the potential of green H₂ in the

heavy transport sector, which could help the latter operate within the SOS for humanity.

Here we assess whether H₂ production via the gasification of wP could operate without exceeding the SOS delimited by the PBs and compare the economic performance and life-cycle impacts of 13 H₂ production routes from an AESA viewpoint through the lens of the PBs.³⁵ The wP deployed in the gasification process is composed of polyethylene (PE), polypropylene (PP), and polystyrene (PS), altogether representing 56% of the total polymer waste in 2015.¹ We found that H₂-from-polymers coupled with CCS outperforms gray and blue H₂, as well as most electrolytic routes in all PBs. Moreover, when considering downscaling, no current technology would be environmentally sustainable, as they all transgress at least one PB due to their carbon emissions, yet a portfolio of them would allow operating sustainably within the downscaled SOS. Our study underlines the importance of employing AESA to drive decision-making in the development of a more sustainable economy.

METHODS DESCRIPTION

We here analyze the environmental sustainability performance of 13 H₂ routes encompassing gray and blue H₂, several green H₂ pathways, and polymer waste gasification (wPG). Our work combines process simulation, a life cycle impact assessment aligned with the PBs framework, and a techno-economic assessment of the wPG processes to elucidate whether this novel route is economically appealing. The following subsections describe the above-mentioned methods.

H₂-from-Polymers–Process Modeling. The H₂-from-polymers process was simulated in Aspen Plus V11, using the RK-SOAVE property method and Redlich–Kwong–Soave cubic equation of state suitable for hydrocarbons and mixtures of mildly polar gases, particularly at high temperatures and pressures.³⁷

We created a flowsheet that produces H₂ at 99.96% purity from wP (Figure 1a).³⁸ The wPG process consists of syngas generation through steam gasification of wP, H₂ production through the water–gas shift (WGS) reaction, and separation via pressure swing adsorption (PSA). The wPG process with CCS (wPG+CCS) comprises an additional unit to compress the CO₂ (Figure 1b). The PSA unit's tail gas is combusted, generating heat for the gasifier. Additionally, we combust 1.5% of the pure H₂ stream to cover the heat demand for wPG (3.5% for wPG+CCS).

We feed 5 t wP h⁻¹ to the gasifier. This value was estimated based on packaging waste data from the United Kingdom, as described in section 3 of the Supporting Information. This mixed stream contains 63.4 wt % PE, 30 wt % PP, and 6.6% PS, based on the output of the sorting facility from Kleinhans et al.³⁹

The gasifier operates at 800 °C and 1.013 bar. It is modeled in Aspen Plus in two steps: wP decomposes in an RYIELD reactor, followed by the steam gasification reaction using low-pressure steam (LP steam) in the conditions indicated in Figure 1a in a RIGIBBS reactor.¹⁸ The resulting syngas is compressed to 32.5 bar through a series of three compressors with intercooling before going to the water–gas shift (WGS) reactors.⁴⁰ The WGS reaction takes place at 32.5 bar in two steps, a high-temperature shift (HT-WGS) at 400 °C with a conversion of 88%, and a low-temperature shift (LT-WGS) at 250 °C, yielding a total CO conversion of 95 mol %.⁴⁰ The resulting stream is cooled to 50 °C and flashed before being sent to the pressure swing adsorption (PSA) unit that separates H₂ with a molar purity of 99.96%.⁴¹ The pure H₂ leaves the process at 50 °C and 31.7 bar.

The tail gas is decompressed and combusted in a furnace (combustion reactor) at 1.5 bar and 1300 °C, which generates heat for the gasification. In the wPG process, this combustion is performed with air, and the postcombustion stream, containing 56.9 mol % CO₂, is vented after cooling and flashing at 40 °C.

In the wPG+CCS configuration, the tail gas undergoes an oxy-fuel combustion with a near stoichiometric equivalence of pure O₂ (same pressure and temperature as the tail gas combustion in the wPG process). After cooling and flashing, the resulting stream, which contains 94.4 mol % CO₂, is sent to an additional unit (Figure 1b). It is compressed in four steps, with intercooling and flashing, to 150 bar and 40 °C for geological storage. The flashed streams are decompressed to 1.013 bar and undergo a final flash (Flash 7). The liquid phase goes to wastewater treatment with the one from Flash 3, and the gaseous phase is recirculated to the combustion chamber.

Heat integration was performed with Aspen Energy Analyzer V11, obtaining a heat exchanger network (HEN) where neither wPG nor wPG+CCS require extra heating utilities. Moreover, LP and HP steam could be generated when cooling hot streams above 135 and 260 °C, respectively, covering the steam needs for the gasification and WGS reaction, while cooling water was used for cooling to temperatures below 135 °C.

Life Cycle Impact Assessment (LCIA). Our study follows the ISO 14040⁴² and ISO 14044⁴³ guidelines. The goal of the study is to quantify the environmental sustainability level of H₂ production in the 13 routes described next. We follow a cradle-to-gate approach, i.e., the system boundaries comprise the life-cycle phases from raw materials extraction to H₂ production, including plant construction. The subsequent use of H₂ is excluded.

Second, the life cycle inventories (LCI) are generated. These include the raw materials, water, energy, and emissions of our systems. We used the Simapro 9.2⁴⁴ software and the Ecoinvent 3.5 database⁴⁵ to generate the LCIs further described in section 2 of the Supporting Information.

In the third LCA phase, we calculated the impacts using two LCIA methodologies. First, we evaluated the GWI of the scenarios according to the IPCC 2013 100a method.⁴⁶ We also applied the

methodology proposed by Ryberg et al.⁴⁷ to express the environmental impacts of the elementary flows of the LCI in terms of the control variables of the PBs defined for the following Earth-system processes: climate change (CC), quantified via the atmospheric CO₂ concentration (CC–CO₂) and energy imbalance at the top of the atmosphere (CC–EI); stratospheric ozone depletion (SOD); ocean acidification (OA); biogeochemical flows, of nitrogen and phosphorus (BGF–N and BGF–P, respectively); land-system change (LSC); and freshwater use (FWU). The characterization factors used to estimate the change in the terrestrial biosphere integrity (CBI) were taken from Galán-Martín et al.,³¹ based on the work by Hanafiah et al.⁴⁸

For each scenario *s*, the environmental impact on Earth-system process *b* (EI_{b,s}) is calculated with eq 1:

$$EI_{b,s} = \sum_{f \in F} I_{s,f} \times CF_{b,f} \times FU \quad \forall b, s \quad (1)$$

where *I*_{*s*,*f*} represents the quantity of elementary flow *f* associated with the production of one kg of H₂ in scenario *s*, *CF*_{*b*,*f*} is the characterization factor of elementary flow *f* and Earth-system process *b*, and *FU* denotes the functional unit.

Guinée et al.⁴⁹ recently highlighted the importance of considering the limitations that come hand-in-hand with the LCA-based AESA method. One limitation of our study is that the *FU* is assumed to remain constant over time and does not account for the variability of the H₂ market throughout the years. Here, the *FU* corresponds to the share of the global production of H₂ that could be covered accordingly from wP through the wPG+CCS process (more details in section 3.b. of the Supporting Information) and is expressed in Mt H₂ y⁻¹. Thus, EI_{b,s} corresponds to the total environmental impact on Earth-system process *b* that is generated by scenario *s* to meet the *FU*.

To perform the AESA, we quantify the transgression level (TL) as follows. For each Earth-system process *b* and scenario *s*, TL_{b,s} is calculated from the corresponding environmental impact (EI_{b,s}) and the share of the SOS (SOS_{*x*,*b*}) attributed to the studied activity *x*. Depending on the type of analysis, TL_{b,s} can be calculated with respect to the global limits (SOS_{GLO,*b*}, the full SOS estimated as the difference between the value of the planetary boundary and the natural background level⁵⁰) or the downscaled SOS attributed to H₂ (SOS_{H₂,wP,*b*}). The general equation is shown in eq 2 below.

$$TL_{b,s} = \frac{EI_{b,s}}{SOS_{x,b}} \quad \forall b, s \quad (2)$$

Ryberg et al.⁵¹ discuss several downscaling approaches to assign shares of the global SOS to products. Such downscaling principles build on the distributive justice theory to assign a fair share of the total SOS_{GLO} to a given activity based on seven dimensions (i.e., currency, pattern, target, geographical scope, temporal scope, constraints, and clauses).

The choice of the downscaling method can heavily influence the results and conclusions of the analysis. Notably, a recent study by Hjalsted et al.⁵² explored the use of different allocation principles and upscaling methods to assign shares of the SOS to three sectors, highlighting the differences between downscaling methods and proposing a framework to transparently assess the environmental sustainability level of process systems. Thus, here we employ two downscaling methods to determine the status of the H₂ market with the PBs framework.

We define the share of the global SOS allocated to H₂ production according to a utilitarian principle (described here) and the grandfathering downscaling method (described in section 4.b. of the Supporting Information). Here, SOS_{H₂,wP,*b*} is calculated by applying eq 3, following a utilitarian downscaling approach⁵¹ based on the global gross value added (GVA_{GLO} = USD 84.1 × 10¹² in 2018⁵³) and the gross value added for H₂ from wP (GVA_{H₂,wP}). In essence, the more the activity contributes to the economy, the more it is allowed to pollute.

$$\text{SOS}_{\text{H}_2, \text{wP}, b} = \text{SOS}_{\text{GLO}, b} \times \frac{\text{GVA}_{\text{H}_2, \text{wP}}}{\text{GVA}_{\text{GLO}}} \forall b \quad (3)$$

Due to a lack of data, we estimate $\text{GVA}_{\text{H}_2, \text{wP}}$ as a fraction of the chemical sector's GVA ($\text{GVA}_{\text{CHEM}} = \text{USD } 5.7 \times 10^{12}$)⁵⁴ using eq 4, which considers the market size of the chemical sector ($\text{USD } 1.1 \times 10^{12}$),⁵⁴ the 2018 global H_2 demand ($\text{USD } 118.1 \times 10^9$),⁵⁵ and the fraction of the 2018 global H_2 demand that wP could cover ($f_{\text{H}_2, \text{wP}} = 79.8\%$, calculated in section 3.c. of the Supporting Information).

$$\text{GVA}_{\text{H}_2, \text{wP}} = \text{GVA}_{\text{CHEM}} \times \frac{\text{market}_{\text{H}_2}}{\text{market}_{\text{CHEM}}} f_{\text{H}_2, \text{wP}} \quad (4)$$

Finally, in the fourth and last phase of the LCA, we evaluate the implications of our scenarios. A $\text{TL}_{b,s}$ value below 1 indicates that scenario s operates within the allocated SOS for Earth-system process b and is deemed sustainable with respect to that PB. Conversely, a $\text{TL}_{b,s}$ value above 1 implies that scenario s transgresses the allocated SOS for Earth-system process b and is, therefore, unsustainable. We consider that for scenario s to be environmentally sustainable, the $\text{TL}_{b,s}$ values across all studied PBs must be less than 1. Nonetheless, the claim that a given scenario is environmentally sustainable should be interpreted with caution, since the PBs of two Earth-system processes, namely atmospheric aerosol loading and novel entities, have not been quantified yet³⁵ and, therefore, were not included in this analysis. Moreover, we clarify that we use downscaling, so the fact that a given activity transgresses a given share of the SOS does not imply that all the anthropogenic activities will jointly transgress the full SOS.

Life Cycle Inventories (LCI). The LCIs combine process simulation data (foreground system) with data from the Ecoinvent 3.5 database (background system), using the allocation method “cut-off by classification”.⁴⁵ We derived the LCIs for wPG and wPG+CCS from the mass and energy balances of the process model. Moreover, we expanded the system boundaries to account for the treatment of waste PE, PP, and PS. Hence, we assume that wP landfilling and incineration are avoided when recycling polymers through wPG and wPG+CCS. We used data from Ecoinvent 3.5 to compute the avoided burdens linked to these activities, considering the following breakdown of wP treatment alternatives in 2015: 55% landfilled, 25.5% incinerated,¹ and the remaining 19.5% recycled. We further assume that the process uses wP that would be sent for incineration and landfilling otherwise, thus avoiding the burdens linked to these waste treatment activities. Moreover, analogous to the poplar feedstock used in the BG and BG+CCS processes, wP does not come free of burdens. Although the system boundaries are cut off where the polymers become waste, the impacts related to collecting, transporting, sorting, and processing the waste are embedded in the wP feedstock.

wPG and wPG+CCS were compared to 11 H_2 production processes (Figure 2) whose inventories were taken from the literature, as described in section 2.b. of the Supporting Information.

Economic Assessment. We compared the scenarios based on their leveled cost of hydrogen (LCOH), following Parkinson et al.²³ The LCOH of wPG and wPG+CCS was calculated as the total annual cost (TAC) per kg of H_2 produced. The TAC is computed as the sum of the annual capital charge (ACC), fixed operational cost (FOC), and variable operational cost (VOC), as shown in eqs 5 and 6.

$$\text{TAC} = \text{ACC} + \text{FOC} + \text{VOC} \quad (5)$$

$$\text{LCOH} = \frac{\text{TAC}}{\text{annual production of } \text{H}_2} \quad (6)$$

The capital cost was calculated using the cost correlations from Onel et al.⁵⁶ for the PSA unit and Sinnott and Towler⁵⁷ for the remaining equipment. The FOC is a function of the total capital cost of the plant and consists of operating expenditures, such as maintenance, labor, land, taxes, insurance, and plant overheads. The VOC includes the prices of raw materials, electricity, and utilities. All

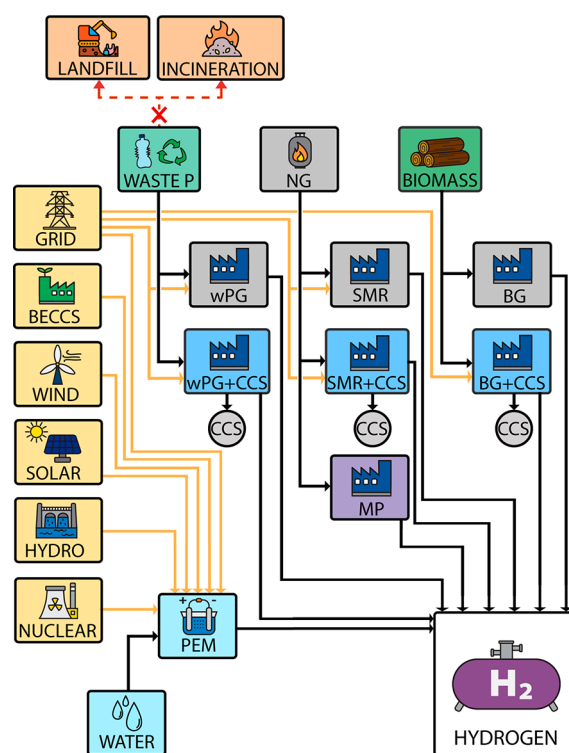


Figure 2. Graphical representation of the studied scenarios. The following acronyms are employed: WASTE P, waste polymers; NG, natural gas; wPG, waste polymers gasification; SMR, steam methane reforming; BG, biomass gasification; CCS, carbon capture and storage; MP, methane pyrolysis; GRID, electricity from the power grid; BECCS, electricity from bioenergy; WIND, electricity from wind power; SOLAR, electricity from photovoltaic cells; HYDRO, hydropower; NUCLEAR, electricity from a nuclear power plant; and PEM, proton exchange membrane electrolysis. The column on the left-hand side of the figure contains the energy sources used for the different technologies. PEM is the only technology that was evaluated with various power sources. The remaining technologies consume electricity coming from the power grid mix of 2018.

costs were expressed in USD 2019, according to the Chemical Engineering Process Cost Index (CEPCI). The list of equipment costs can be found in section 5.a. of the Supporting Information.

RESULTS AND DISCUSSION

First, we discuss the GWI results, and then the impacts on the Earth-system processes, followed by the economic assessment and a cost-optimized portfolio of H_2 technologies to meet the demand within PBs.

Global Warming Impacts (GWI). Figure 3 shows the GWI of the 13 scenarios. The technologies involving biomass coupled to CCS (PEM-BECCS and BG+CCS) are the most favorable, followed by PEM-nuclear, BG, wPG+CCS, PEM-wind, PEM-hydro, MP, PEM-solar, SMR+CCS, wPG, SMR, and PEM-2018 grid mix. Technologies relying on the CCS of biogenic carbon lead to carbon-negative H_2 , preventing net GWI (i.e., PEM-BECCS with a GWI of $-101.12 \text{ kg CO}_2\text{-eq kg}^{-1} \text{ H}_2$ and BG+CCS with a GWI of $-13.80 \text{ kg CO}_2\text{-eq kg}^{-1} \text{ H}_2$). The biomass gasification and combustion processes release the carbon captured by the biomass feedstock during photosynthesis. Thus, processes employing biogenic CO_2 coupled with CCS generate negative emissions, as the biogenic CO_2 is stored underground instead of released into the atmosphere. Figure 3 shows that BG+CCS has net-negative

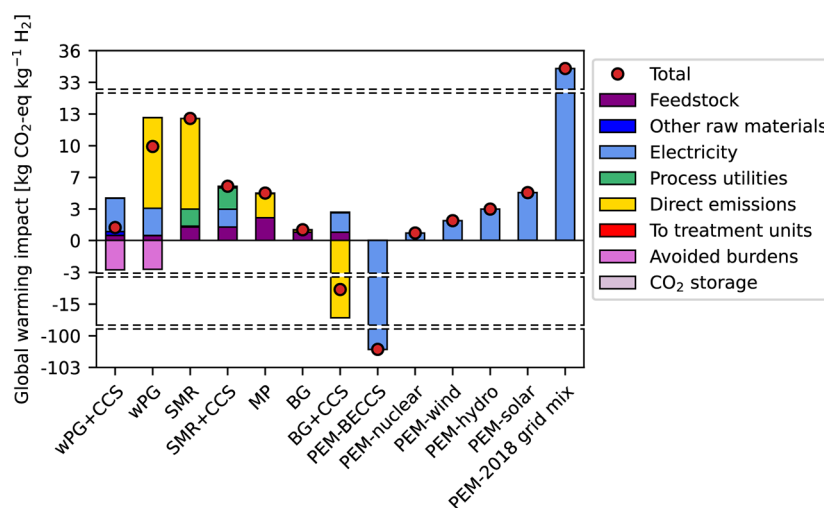


Figure 3. Global warming impact breakdown of the studied H_2 production routes. The following acronyms are employed: wPG, waste polymers gasification; CCS, carbon capture and storage; SMR, steam methane reforming; MP, methane pyrolysis; BG, biomass gasification; PEM, proton exchange membrane electrolysis; BECCS, bioenergy with CCS; nuclear, nuclear power plant; wind, wind power; hydro, hydropower; solar, photovoltaic energy; and 2018 grid mix, electricity from the power grid of 2018.

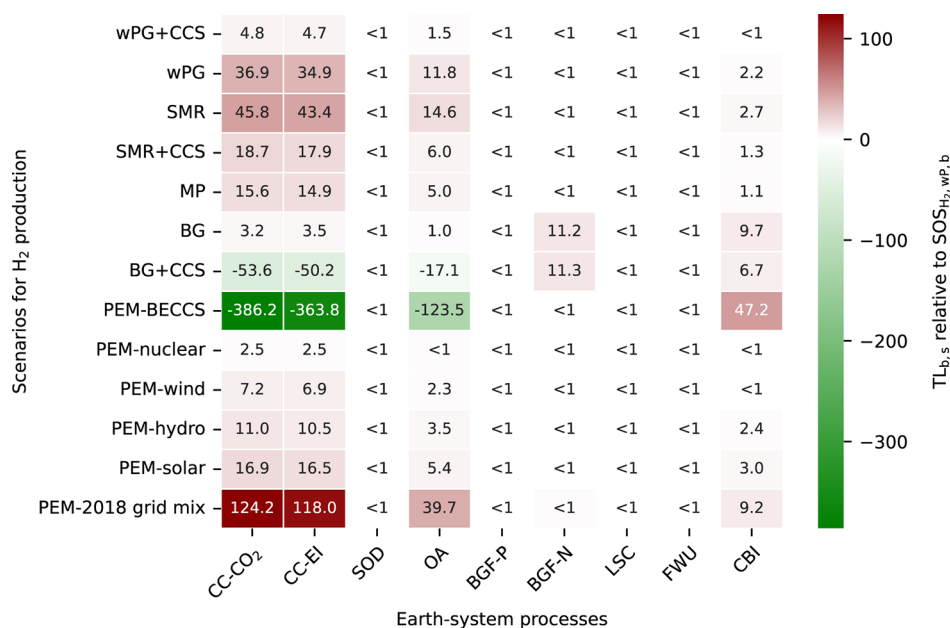


Figure 4. Planetary boundaries assessment of the 13 H_2 production routes. TL relative to $SOS_{H_2,wp,b}$ of the different H_2 routes; values labeled as “<1” indicate that the scenario in question has not transgressed $SOS_{H_2,wp,b}$; negative values (in green) indicate prevented impacts due to avoided burdens and/or capture and storage of biogenic CO_2 ; the remaining values that range from white to red indicate the TL relative to the corresponding SOS associated with each scenario. The following abbreviations are employed: $SOS_{H_2,wp,b}$, safe operating space for Earth-system process b downscaled to the maximum H_2 production from waste polymers (wP); CC, climate change; CO_2 , atmospheric CO_2 concentration; EI, energy imbalance at the top of the atmosphere; SOD, stratospheric ozone depletion; OA, ocean acidification; BGF, biogeochemical flows; P, phosphorus; N, nitrogen; LSC, land-system change; FWU, freshwater use; CBI, change in terrestrial biosphere integrity; wPG, waste polymers gasification; CCS, carbon capture and storage; SMR, steam methane reforming; MP, methane pyrolysis; BG, biomass gasification; PEM, proton exchange membrane electrolysis; BECCS, bioenergy with CCS; nuclear, nuclear power plant; wind, wind power; hydro, hydropower; solar, photovoltaic energy; and 2018 grid mix, electricity from the power grid of 2018.

emissions, whereas the total GWI of BG is positive (1.11 kg CO_2 -eq $kg^{-1} H_2$). In the latter, 77% of the total emissions come from the feedstock (poplar chips), which has embodied GHG emissions due to the planting, harvesting, treating, and transporting steps.

The two processes producing H_2 through chemical recycling, wPG, and wPG+CCS avoid 2.42 kg CO_2 -eq $kg^{-1} H_2$ due to the diversion of wP from incineration and landfill.

The H_2 produced via wPG presents high GWI (9.75 kg CO_2 -eq $kg^{-1} H_2$), still better than SMR (12.66 kg CO_2 -eq $kg^{-1} H_2$). Direct emissions represent the main source of impact in the wPG process; wP contains 89 wt % of carbon, which is released as CO_2 . Although the C:H ratio of methane is smaller, SMR also releases significant amounts of CO_2 . Coupling it to CCS (SMR+CCS, 5.62 kg CO_2 -eq $kg^{-1} H_2$) increases the electricity

and utilities needs but halves the overall GWI by avoiding direct emissions.

wPG+CCS, on the other hand, attains the fifth-lowest GWI (1.34 kg CO₂-eq kg⁻¹ H₂), outperforming the aforementioned scenarios (wPG, SMR, SMR+CCS), MP, and several electrolytic routes (PEM-hydro, PEM-solar, PEM-wind, and PEM-2018 grid mix). The main contributor to the GWI of wPG+CCS is the electricity needed for the syngas and CO₂ compressors (Figure 3). This electricity comes from the 2018 global grid mix, still heavily reliant on fossil fuels.²² Hence, the GWI of this route would significantly drop by using renewables or a cleaner energy mix. For instance, PEM-2018 grid mix, which uses the same 2018 average grid mix, and PEM-wind have very different GWI for similar energy requirements due to the disparity in the carbon intensity of the power sources used.

The GWI of PEM-wind (2.05 kg CO₂-eq kg⁻¹ H₂), PEM-hydro (3.25 kg CO₂-eq kg⁻¹ H₂), and PEM-solar (4.96 kg CO₂-eq kg⁻¹ H₂) are mostly linked to their infrastructure. Specifically, the impacts of hydropower are linked to dam construction. The GWI of solar power stems from the energy and materials embodied in photovoltaic panels. Similarly, wind power embeds the impacts of mining and treatment of the materials used in the turbines and their construction.⁵⁸ PEM-nuclear (0.77 kg CO₂-eq kg⁻¹ H₂) presents lower GWI than most studied technologies, except for PEM-BECCS and BG+CCS. Nuclear energy performs better in global warming than other power technologies, and its emissions are mostly related to the mining and refining of uranium and the material and energy requirements for building the nuclear reactor.

Overall, wPG+CCS shows lower GWI than SMR, SMR+CCS, MP, and most electrolytic routes but still higher than technologies involving biomass coupled with CCS. We next discuss the AESA results complementing the GWI analysis.

Planetary Boundaries Analysis. The PB results are expressed considering as the functional unit the total amount of H₂ that could be produced in one year from the global amount of wPE, wPP, and wPS generated in 2018 (79.8% of the global demand for pure H₂ in 2018, corresponding to 58.9 Mt H₂ y⁻¹). To achieve net-zero CO₂ emissions by 2050, the International Energy Agency (IEA) estimated that the global demand for H₂ and H₂-based fuels will increase from less than 90 Mt in 2020 to 530 Mt in 2050, at a rate of ca. 6% per year.⁵⁹ In contrast, future wP generation is expected to increase at a slower rate, of 2.17% per year (from 60 to 99 Mt in 2015 to 155–265 Mt in 2060).⁶⁰ Thus, H₂-from-polymers could not cover the current or future H₂ demand alone.

Figure 4 presents the impacts of the 13 technologies on seven Earth-system processes: climate change (CC), considering atmospheric CO₂ concentration (CC-CO₂) and energy imbalance at the top of the atmosphere (CC-EI) as control variables; stratospheric ozone depletion (SOD); ocean acidification (OA); biogeochemical flows, phosphorus (BGF-P) and nitrogen (BGF-N); land-system change (LSC); freshwater use (FWU); and change in the terrestrial biosphere integrity (CBI). The impacts are expressed as the TL relative to the downscaled SOS defined for each Earth-system process (SOS_{H₂,wP,b}).

The results show that none of the scenarios transgress the full SOS, SOS_{GLO}, for any Earth-system processes (Figure S1). However, none of the scenarios is deemed environmentally sustainable when calculating the TL relative to the SOS

attributed to H₂ (SOS_{H₂,wP,b}), i.e., only 0.07% of SOS_{GLO} following the utilitarian sharing principle (Figure 4). The H₂ routes affect mostly the CC Earth-system process, where the TL for SOS_{H₂,wP,CC-CO₂} and SOS_{H₂,wP,CC-EI} ranges from -386.2 to 124.2 and from -363.8 to 118.0, respectively. Furthermore, the impacts on OA (TL_{OA,b} relative to SOS_{H₂,wP,OA} ranging between -123.5 and 39.7) follow similar trends since they are also primarily dictated by the atmospheric CO₂ concentration.³⁴

The wPG+CCS scenario outperforms SMR, SMR+CCS, MP, and several electrolytic routes (i.e., PEM-hydro, PEM-solar, PEM-wind, and PEM-2018 grid mix) in all impact categories. The lack of direct emissions from the wPG+CCS process and the avoided burdens from the incineration and landfilling of the polymers lead to these favorable results. In turn, wPG only performs slightly better than SMR since, despite the higher electricity needs of wPG, the avoided burdens linked to the alternative polymer end-of-life treatments determine its better performance.

The reason why none of the studied scenarios remains within the downscaled ecological budget SOS_{H₂,wP,b} is mostly because of their high impacts on CC, OA, and terrestrial biosphere integrity. The technologies sequestering biogenic CO₂ prevent CC and OA impacts due to their negative carbon balance, whereas the other H₂ production routes transgress the downscaled SOS in CC and OA (except for PEM-nuclear, which does not exceed the OA budget). On the downside, BG and BG+CCS worsen the biogeochemical nitrogen flow (downscaled TL_{BGF-N,b} of 11.2 for BG and 11.3 for BG+CCS, vs <1 in the SMR) due to fertilizers use. Moreover, the processes deploying biomass (PEM-BECCS, BG, and BG+CCS) exert substantial pressure on the CBI Earth-system process (transgressing SOS_{H₂,wP,CBI} up to 47.2 times with PEM-BECCS) due to the significant land requirements of poplar.

Despite all the scenarios transgressing at least one downscaled PB, none transgresses any of the following four Earth-system processes: SOD, BGF-P, LSC, and FWU. Moreover, only two H₂ production routes transgress the allocated budget for the N flows (i.e., BG, and BG+CCS from highest to lowest TL, respectively). Remarkably, the biomass scenarios do not exceed the land-system change PB because we assume that the biomass plantations are not deployed on forested land, the only land type covered by the LSC PB control variable.

Moreover, wPG+CCS, PEM-nuclear, and PEM-wind are the only scenarios not transgressing the terrestrial biosphere integrity budget SOS_{H₂,wP,CBI}. The impacts on the CBI Earth-system process are linked to land use and GHG emissions.^{31,48} Therefore, the biomass scenarios present the highest TL in this category, together with the PEM-2018 grid mix scenario. Although the latter shows a low impact on five Earth-system processes (i.e., SOD, BGF-P, BGF-N, LSC, and FWU), it generates substantial impacts on the Earth-system processes linked to CO₂ emissions because it relies on a power mix yet to be decarbonized. Indeed, it presents the highest TL among all scenarios for CC-CO₂, CC-EI, and OA, due to the heavy reliance of the 2018 average energy mix on fossil fuels.⁶¹

In summary, although all scenarios operate within the global limits of the PBs framework, none of them can be deemed environmentally sustainable when considering downscaling, as

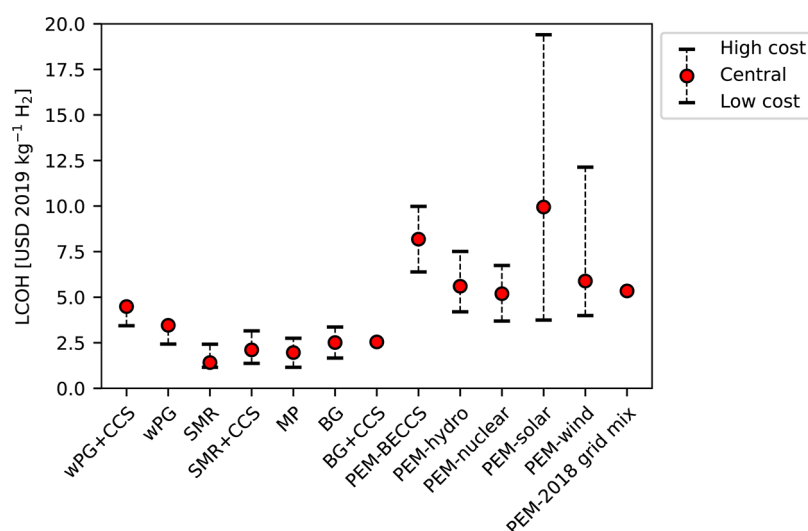


Figure 5. Levelized cost of hydrogen (LCOH) for the alternative production routes, expressed in USD 2019 $\text{kg}^{-1} \text{H}_2$. All values of LCOH consider the CAPEX and OPEX of the technology in question, including the pre-energy crisis literature estimates by Parkinson et al.²³ wPG and wPG+CCS have only central and low LCOH, accounting, respectively, to the cases where the wP feedstock are costly and free. All values were normalized to USD 2019, using the CEPCI.

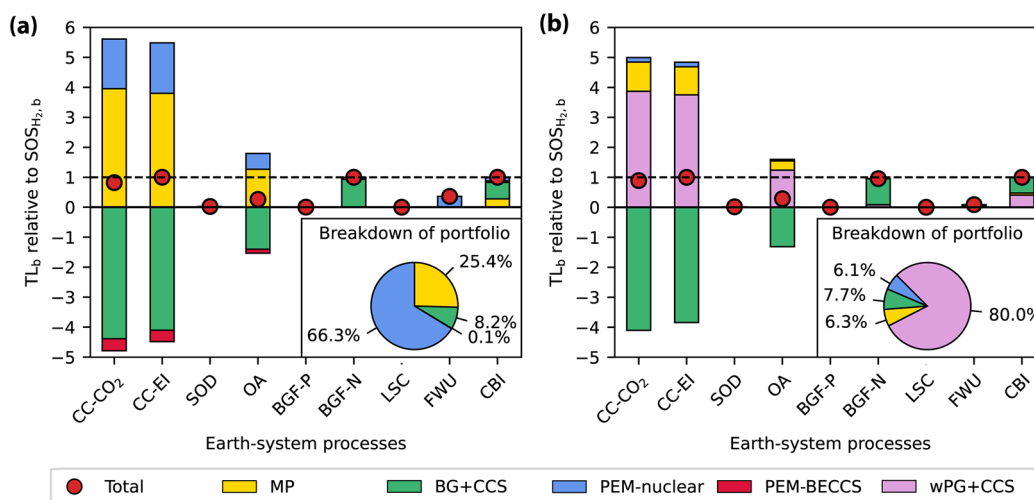


Figure 6. Results of the cost optimization of global H_2 production within planetary boundaries. (a) Case for a high cost of waste polymers. (b) Case where waste polymers are free. Bar plots showcase the contribution of the individual technologies of the optimal portfolio to the transgression level (TL_b) relative to the downscaled safe operating space attributed to the global H_2 demand ($\text{SOS}_{\text{H}_2,b}$) for each Earth-system process b . $\text{TL}_b \leq 1$ indicates that the downscaled SOS defined for Earth-system process b has not been transgressed. The dashed line corresponds to $\text{TL}_b = 1$. Pie charts display the contribution of the H_2 technologies to the optimal H_2 portfolio.

they exceed the allocated $\text{SOS}_{\text{H}_2,\text{wP},b}$ for at least one of the seven studied Earth-system processes.

Economic Assessment and LCOH. The costs of H_2 from wPG and wPG+CCS were estimated at 3.46 USD $\text{kg}^{-1} \text{H}_2$ and 4.49 USD $\text{kg}^{-1} \text{H}_2$, respectively (cost breakdown in Figure S2). In both cases, the annualized capital expenditures (CAPEX) dominate the total cost (55.1% for wPG and 51.1% for wPG+CCS). Another important cost driver is the wP feedstock, on average traded for 308.3 € t^{-1} wPE, 354.4 € t^{-1} wPP, and 411.1 € t^{-1} wPS within the European Union in 2019.⁶² For this analysis, these were converted to USD, applying a 1.1 USD €^{-1} conversion. The costs are specific to the European Union and, therefore, might vary for other countries. These high costs are related to the collection, sorting, and transport to processing facilities.⁶³

To contextualize these costs, we compared them against the LCOH of the other 11 technologies (Figure 5, costs calculated as described in eq 6, taking into account their CAPEX and OPEX and the data and assumptions in Tables S3 and S4). The LCOH of SMR, SMR+CCS, MP, BG, BG+CCS, PEM-nuclear, PEM-wind, and PEM-solar are literature estimates reported by Parkinson et al.²³

Both wPG and wPG+CCS are more costly than SMR, SMR+CCS, MP, BG, and BG+CCS, being only cheaper than the central estimate (median) of the electrolytic routes. The wPG process could compete with SMR if wP were free, which would lead to a 29.8% reduction of the LCOH, reaching the highest cost reported for SMR (2.43 USD $\text{kg}^{-1} \text{H}_2$). Analogously, the LCOH of wPG+CCS would drop to 3.44 USD $\text{kg}^{-1} \text{H}_2$, becoming comparable to the upper bound for BG (3.36 USD $\text{kg}^{-1} \text{H}_2$) and SMR+CCS (3.36 USD $\text{kg}^{-1} \text{H}_2$). Additionally,

integrating wPG+CCS routes into ammonia production plants, which traditionally deploy SMR to generate H₂, could further reduce the H₂ production cost. Notably, the air separation unit could simultaneously supply the oxygen required for the oxy-combustion of the tail gas within the wPG+CCS process and the nitrogen feedstock to the Haber-Bosch process, thereby reducing the overall expenses.

In summary, H₂-from-polymers is cheaper than electrolytic H₂ but more expensive than biomass- and fossil-based routes.

Meeting the Global H₂ Demand within PBs. We showed that no single technology could meet the global H₂ demand within PBs when considering downscaling. Moreover, although H₂ from wPG+CCS performs better than the fossil routes SMR and SMR+CCS, it is not economically competitive due to the high wP cost. Thus, we performed a cost optimization considering pre-energy crisis data to determine whether an optimal combination of technologies could meet the global H₂ demand within downscaled PBs (details in section 6 of the [Supporting Information](#)). This is not intended to be an exhaustive optimization, which should consider regionalized data and technical constraints to model the feasibility of the power mix supplying energy to the electrolytic routes. Instead, we perform a simplified analysis to shed light on whether the hybridization of technologies could, in principle, allow covering the H₂ demand within downscaled PBs; further analyses based on a more detailed model should complement these preliminary results.

The optimization revealed that the total global annual H₂ production of 73.9 Mt H₂ could be met without transgressing the downscaled SOS by combining 66.3 wt % of PEM-nuclear-H₂, 25.4 wt % MP-H₂, 8.2 wt % BG+CCS-H₂, and 0.1 wt % PEM-BECCS-H₂. The H₂ cost in this portfolio would be 4.16 USD kg⁻¹ H₂ (vs 1.41 USD kg⁻¹ H₂ in the BAU), with a total cost of H₂ production adding up to USD 307.5 × 10⁹, which corresponds to 2.6 times the market value of the 2018 global H₂ demand (USD 118.1 × 10⁹).⁵⁵ The breakdown of the total TL with respect to the downscaled SOS for each Earth-system processes is shown in [Figure 6a](#).

A second case was considered, assuming that wP would be free. In this case, the H₂-from-wPG+CCS cost would drop to 3.44 USD kg⁻¹ H₂, and H₂ from wP would appear in the portfolio designed to cover the same demand within PBs, i.e., 80.0 wt % of the total H₂ through wPG+CCS, 6.1 wt % through PEM-nuclear, 7.7 wt % through BG+CCS, and 6.3 wt % through MP ([Figure 6b](#)). The total cost of this technology portfolio would be USD 250.0 × 10⁹ (3.38 USD kg⁻¹ H₂), corresponding to 2.1 times the market value of the 2018 global H₂ demand.

Moreover, the second portfolio, which was optimized considering free wP, would still yield a competitive H₂ price relative to the minimum cost one ([Figure 6a](#)) within PBs even assuming a high cost of the wP (multiplying the proportions corresponding to each technology of the portfolio of [Figure 6b](#) by their LCOH, considering a value for wPG+CCS where wP is costly, we would get a cost of USD 312.1 × 10⁹ or 4.22 USD kg⁻¹ H₂ (vs 4.16 USD kg⁻¹ H₂ in [Figure 6a](#)). As we discuss in section 7 of the [Supporting Information](#), the technologies deploying wP become more competitive if externalities are considered, supporting the claim that H₂ from wP could play a role in future H₂ portfolios, even without government subsidies.

CONCLUSIONS

In this work, we compared H₂ from waste polymers with 11 H₂ production routes, finding that it could substantially reduce the carbon footprint and carbon-related PBs impact of gray H₂ while outperforming most electrolytic routes. All the H₂ routes explored here would be unsustainable when considering downscaling because, although they do not transgress any of the global SOS by itself, they exceed the downscaled SOS defined by at least one PB (primarily climate change in most cases and terrestrial biosphere integrity in the biomass pathways).

Additionally, we found that wP pathways to H₂ are not economically competitive against the fossil routes due to their high CAPEX and wP costs, despite being cheaper than the electrolytic pathways. Moreover, wPG+CCS would require permanent storage of the captured CO₂.

The portfolio optimization considering pre-energy crisis data revealed that it would be possible to fully cover the current global demand of H₂ without transgressing any downscaled PBs by hybridizing technologies based on fossil and renewable resources. Although the minimum cost solution operating within the PBs would not involve H₂-from-polymers in the current state, wPG+CCS would appear in the mix if the wP feedstock was free. However, the cost of achieving a H₂ economy that operates within PBs, using the technologies assessed here, would be significantly higher than the current market value. The increase in the cost of fossil resources due to the current geopolitical scenario may nonetheless improve the economic appeal of the renewable routes, modifying the economic ranking of technologies. Moreover, the need to reduce the dependency on fossil resources for energy security issues may further favor the renewable technologies.

Overall, this work demonstrates that H₂-from-polymers could help to operate within the PBs. Using wP as both a carbon and H₂ source for chemicals production might be the way forward, yet converting it into H₂ until chemical recycling reaches a sufficient maturity level could be a promising interim solution. Hence, deploying this technology in tandem with other recycling processes and exploring its hybridization with other H₂ pathways could facilitate the transition toward a more sustainable economy.

ASSOCIATED CONTENT

Supporting Information

The Supporting Information is available free of charge at <https://pubs.acs.org/doi/10.1021/acssuschemeng.2c05729>.

Information on the life cycle inventories created for this study, the assumptions made, details on cost calculations, and the description of the optimization problem ([PDF](#))

AUTHOR INFORMATION

Corresponding Author

Gonzalo Guillén-Gosálbez – *Institute for Chemical and Bioengineering, Department of Chemistry and Applied Biosciences, ETH Zürich, 8093 Zürich, Switzerland;*

orcid.org/0000-0001-6074-8473;

Email: gonzalo.guillen.gosalbez@chem.ethz.ch

Authors

Cecilia Salah – *Institute for Chemical and Bioengineering, Department of Chemistry and Applied Biosciences, ETH*

Zürich, 8093 Zürich, Switzerland; orcid.org/0000-0002-3376-706X

Selene Cobo – Institute for Chemical and Bioengineering, Department of Chemistry and Applied Biosciences, ETH Zürich, 8093 Zürich, Switzerland; orcid.org/0000-0002-2879-6261

Javier Pérez-Ramírez – Institute for Chemical and Bioengineering, Department of Chemistry and Applied Biosciences, ETH Zürich, 8093 Zürich, Switzerland; orcid.org/0000-0002-5805-7355

Complete contact information is available at:
<https://pubs.acs.org/10.1021/acssuschemeng.2c05729>

Notes

The authors declare no competing financial interest.

ACKNOWLEDGMENTS

This publication was created as part of NCCR Catalysis (Grant no. 180544), a National Centre of Competence in Research funded by the Swiss National Science Foundation.

REFERENCES

- (1) Geyer, R.; Jambeck, J. R.; Law, K. L. Production, Use, and Fate of All Plastics Ever Made. *Sci. Adv.* **2017**, *3* (7), 1.
- (2) Ellen MacArthur Foundation. The New Plastics Economy: Rethinking the Future of Plastics. 2016. <https://ellenmacarthurfoundation.org/the-new-plastics-economy-rethinking-the-future-of-plastics> (accessed 2023-01-20).
- (3) Lebreton, L.; Slat, B.; Ferrari, F.; Sainte-Rose, B.; Aitken, J.; Marthouse, R.; Hajbane, S.; Cunsolo, S.; Schwarz, A.; Levivier, A.; Noble, K.; Debeljak, P.; Maral, H.; Schoeneich-Argent, R.; Brambini, R.; Reisser, J. Evidence That the Great Pacific Garbage Patch Is Rapidly Accumulating Plastic. *Sci. Rep.* **2018**, *8* (1), 1–15.
- (4) Okunola A, A.; Kehinde I, O.; Oluwaseun, A.; Olufiropo E, A. Public and Environmental Health Effects of Plastic Wastes Disposal: A Review. *J. Toxicol. Risk Assess.* **2019**, *5* (2), 1.
- (5) Ilyas, M.; Ahmad, W.; Khan, H.; Yousaf, S.; Khan, K.; Nazir, S. Plastic Waste as a Significant Threat to Environment - A Systematic Literature Review. *Rev. Environ. Health* **2018**, *33* (4), 383–406.
- (6) Ahmed, T.; Shahid, M.; Azeem, F.; Rasul, I.; Shah, A. A.; Noman, M.; Hameed, A.; Manzoor, N.; Manzoor, I.; Muhammad, S. Biodegradation of Plastics: Current Scenario and Future Prospects for Environmental Safety. *Environ. Sci. Pollut. Res.* **2018**, *25* (8), 7287–7298.
- (7) Yang, X.; Bento, C. P. M.; Chen, H.; Zhang, H.; Xue, S.; Lwanga, E. H.; Zomer, P.; Ritsema, C. J.; Geissen, V. Influence of Microplastic Addition on Glyphosate Decay and Soil Microbial Activities in Chinese Loess Soil. *Environ. Pollut.* **2018**, *242*, 338–347.
- (8) Meys, R.; Katelhon, A.; Bachmann, M.; Winter, B.; Zibunas, C.; Suh, S.; Bardow, A. Achieving Net-Zero Greenhouse Gas Emission Plastics by a Circular Carbon Economy. *Science (80-.)* **2021**, *374*, 71–76.
- (9) van der Hulst, M. K.; Ottenbros, A. B.; van der Drift, B.; Ferjan, Š.; van Harmelen, T.; Schwarz, A. E.; Worrell, E.; van Zelm, R.; Huijbregts, M. A. J.; Hauck, M. Greenhouse Gas Benefits from Direct Chemical Recycling of Mixed Plastic Waste. *Resour. Conserv. Recycl.* **2022**, *186*, 106582.
- (10) Jehanno, C.; Alty, J. W.; Roosen, M.; De Meester, S.; Dove, A. P.; Chen, E. Y. X.; Leibfarth, F. A.; Sardon, H. Critical Advances and Future Opportunities in Upcycling Commodity Polymers. *Nature* **2022**, *603* (7903), 803–814.
- (11) Schwarz, A. E.; Ligthart, T. N.; Godoi Bizarro, D.; De Wild, P.; Vreugdenhil, B.; van Harmelen, T. Plastic Recycling in a Circular Economy; Determining Environmental Performance through an LCA Matrix Model Approach. *Waste Manag.* **2021**, *121*, 331–342.
- (12) Bora, R. R.; Wang, R.; You, F. Waste Polypropylene Plastic Recycling toward Climate Change Mitigation and Circular Economy: Energy, Environmental, and Technoeconomic Perspectives. *ACS Sustain. Chem. Eng.* **2020**, *8* (43), 16350–16363.
- (13) Zhao, X.; You, F. Consequential Life Cycle Assessment and Optimization of High-Density Polyethylene Plastic Waste Chemical Recycling. *ACS Sustain. Chem. Eng.* **2021**, *9* (36), 12167–12184.
- (14) Somoza-Tornos, A.; Gonzalez-Garay, A.; Pozo, C.; Graells, M.; Espuña, A.; Guillén-Gosálbez, G. Realizing the Potential High Benefits of Circular Economy in the Chemical Industry: Ethylene Monomer Recovery via Polyethylene Pyrolysis. *ACS Sustain. Chem. Eng.* **2020**, *8* (9), 3561–3572.
- (15) Conesa, J. A.; Font, R.; Marcilla, A.; Caballero, J. A. Kinetic Model for the Continuous Pyrolysis of Two Types of Polyethylene in a Fluidized Bed Reactor. *J. Anal. Appl. Pyrolysis* **1997**, *40–41*, 419–431.
- (16) Pires Costa, L.; Vaz De Miranda, D. M.; Pinto, J. C. Critical Evaluation of Life Cycle Assessment Analyses of Plastic Waste Pyrolysis. *ACS Sustain. Chem. Eng.* **2022**, *10* (12), 3799–3807.
- (17) Das, S.; Liang, C.; Dunn, J. B. Plastics to Fuel or Plastics: Life Cycle Assessment-Based Evaluation of Different Options for Pyrolysis at End-of-Life. *Waste Manag.* **2022**, *153*, 81–88.
- (18) Saebea, D.; Ruengrit, P.; Arpornwichanop, A.; Patcharavorachot, Y. Gasification of Plastic Waste for Synthesis Gas Production. *Energy Reports* **2020**, *6*, 202–207.
- (19) Gungor, B.; Dincer, I. Development of a Waste-to-Energy Gasification System for Sustainable Communities. *Int. J. Energy Res.* **2022**, *46* (14), 20704–20717.
- (20) Janajreh, I.; Adeyemi, I.; Elagroudy, S. Gasification Feasibility of Polyethylene, Polypropylene, Polystyrene Waste and Their Mixture: Experimental Studies and Modeling. *Sustain. Energy Technol. Assessments* **2020**, *39* (March), 100684.
- (21) International Energy Agency (IEA). The Future of Hydrogen. 2019. <https://www.iea.org/reports/the-future-of-hydrogen> (accessed 2022-12-10).
- (22) International Energy Agency (IEA). Greenhouse Gas Emissions from Energy: Overview. 2021. <https://www.iea.org/reports/greenhouse-gas-emissions-from-energy-overview> (accessed 2022-12-10).
- (23) Parkinson, B.; Balcombe, P.; Speirs, J. F.; Hawkes, A. D.; Hellgardt, K. Levelized Cost of CO₂ Mitigation from Hydrogen Production Routes. *Energy Environ. Sci.* **2019**, *12* (1), 19–40.
- (24) Al-Qahtani, A.; Parkinson, B.; Hellgardt, K.; Shah, N.; Guillén-Gosálbez, G. Uncovering the True Cost of Hydrogen Production Routes Using Life Cycle Monetisation. *Appl. Energy* **2021**, *281*, 115958.
- (25) Verma, A.; Kumar, A. Life Cycle Assessment of Hydrogen Production from Underground Coal Gasification. *Appl. Energy* **2015**, *147*, 556–568.
- (26) Bhandari, R.; Trudewind, C. A.; Zapp, P. Life Cycle Assessment of Hydrogen Production via Electrolysis - A Review. *J. Clean. Prod.* **2014**, *85*, 151–163.
- (27) Lan, K.; Yao, Y. Feasibility of Gasifying Mixed Plastic Waste for Hydrogen Production and Carbon Capture and Storage. *Commun. Earth Environ.* **2022**, *3* (3), 300.
- (28) Cobo, S.; Dominguez-Ramos, A.; Irabien, A. From Linear to Circular Integrated Waste Management Systems: A Review of Methodological Approaches. *Resour. Conserv. Recycl.* **2018**, *135*, 279–295.
- (29) Bakshi, B. R.; Gutowski, T. G.; Sekulic, D. P. Claiming Sustainability: Requirements and Challenges. *ACS Sustain. Chem. Eng.* **2018**, *6* (3), 3632–3639.
- (30) González-Garay, A.; Frei, M. S.; Al-Qahtani, A.; Mondelli, C.; Guillén-Gosálbez, G.; Pérez-Ramírez, J. Plant-to-Planet Analysis of CO₂-Based Methanol Processes. *Energy Environ. Sci.* **2019**, *12* (12), 3425–3436.
- (31) Galán-Martín, Á.; Tulus, V.; Díaz, I.; Pozo, C.; Pérez-Ramírez, J.; Guillén-Gosálbez, G. Sustainability Footprints of a Renewable

Carbon Transition for the Petrochemical Sector within Planetary Boundaries. *One Earth* **2021**, *4* (4), 565–583.

(32) D'Angelo, S. C.; Cobo, S.; Tulus, V.; Naber, A.; Martín, A. J.; Pérez-Ramírez, J.; Guillén-Gosálbez, G. Planetary Boundaries Analysis of Low-Carbon Ammonia Production Routes. *ACS Sustain. Chem. Eng.* **2021**, *9* (29), 9740–9749.

(33) Bjorn, A.; Chandrakumar, C.; Boulay, A. M.; Doka, G.; Fang, K.; Gondran, N.; Hauschild, M. Z.; Kerkhof, A.; King, H.; Margni, M.; McLaren, S.; Mueller, C.; Owsianiak, M.; Peters, G.; Roos, S.; Sala, S.; Sandin, G.; Sim, S.; Vargas-Gonzalez, M.; Ryberg, M. Review of Life-Cycle Based Methods for Absolute Environmental Sustainability Assessment and Their Applications. *Environ. Res. Lett.* **2020**, *15* (8), 083001.

(34) Rockström, J.; Steffen, W.; Noone, K.; Persson, Å.; Chapin, F. S.; Lambin, E. F.; Lenton, T. M.; Scheffer, M.; Folke, C.; Schellnhuber, H. J.; Nykvist, M.; De Wit, C. A.; Hughes, T.; Van Der Leeuw, S.; Rodhe, H.; Sörlin, S.; Snyder, P. K.; Costanza, R.; Svedin, U.; Falkenmark, M.; Karlberg, L.; Corell, R. W.; Fabry, V. J.; Hansen, J.; Walker, B.; Liverman, D.; Richardson, K.; Crutzen, P.; Foley, J. A. Planetary Boundaries: Exploring the Safe Operating Space for Humanity. *Ecol. Soc.* **2009**, *14*, 1.

(35) Steffen, W.; Richardson, K.; Rockström, J.; Cornell, S. E.; Fetzer, I.; Bennett, E. M.; Biggs, R.; Carpenter, S. R.; De Vries, W.; De Wit, C. A.; Folke, C.; Gerten, D.; Heinke, J.; Mace, G. M.; Persson, L. M.; Ramanathan, V.; Reyers, B.; Sörlin, S. Planetary Boundaries: Guiding Human Development on a Changing Planet. *Science* (80-). **2015**, *347* (6223), 1259855.

(36) Valente, A.; Tulus, V.; Galán-Martín, Á.; Huijbregts, M. A. J.; Guillén-Gosálbez, G. The Role of Hydrogen in Heavy Transport to Operate within Planetary Boundaries. *Sustain. Energy Fuels* **2021**, *5* (18), 4637–4649.

(37) AspenTech. Physical Property Methods and Models 11.1. 2001. <https://www.aspentech.com/en/products/engineering/aspens-plus> (accessed 2022–12–20).

(38) Salah, C.; Cobo, S.; Guillén-Gosálbez, G. Assessing the Environmental Potential of Hydrogen from Waste Polyethylene. *Comput.-Aided Chem. Eng.* **2022**, *49* (3), 1933–1938.

(39) Kleinhans, K.; Halleman, M.; Huysveld, S.; Thomassen, G.; Ragaert, K.; Van Geem, K. M.; Roosen, M.; Mys, N.; Dewulf, J.; De Meester, S. Development and Application of a Predictive Modelling Approach for Household Packaging Waste Flows in Sorting Facilities. *Waste Manag.* **2021**, *120*, 290–302.

(40) Luyben, W. L. Plantwide Control of a Coupled Reformer/Ammonia Process. *Chem. Eng. Res. Des.* **2018**, *134*, 518–527.

(41) Susmozas, A. I. Analysis of Energy Systems Based on Biomass Gasification. (Doctoral thesis Universidad Rey Juan Carlos) 2015, Retrieved from BURJC-Digital database. <https://burjcdigital.urjc.es/handle/10115/13599> (accessed 2022–12–2022).

(42) International Standards Organization (ISO). ISO 14040: Environmental management - Life Cycle Assessment - Principles and Framework. 2006. <https://www.iso.org/standard/37456.html> (accessed 2022–12–20).

(43) International Standards Organization (ISO). ISO 14044: Environmental Management - Life Cycle Assessment - Requirements and Guidelines. 2006. <https://www.iso.org/standard/38498.html> (accessed 2022–12–20).

(44) SimaPro. <https://simapro.com/> (accessed 2022–12–10).

(45) Wernet, G.; Bauer, C.; Steubing, B.; Reinhard, J.; Moreno-Ruiz, E.; Weidema, B. The Ecoinvent Database Version 3 (Part I): Overview and Methodology. *Int. J. Life Cycle Assess.* **2016**, *21* (9), 1218–1230.

(46) Intergovernmental Panel on Climate Change (IPCC). 2013 Revised Supplementary Methods and Good Practice Guidance Arising from the Kyoto Protocol. 2014. <https://www.ipcc.ch/publication/2013-revised-supplementary-methods-and-good-practice-guidance-arising-from-the-kyoto-protocol/> (accessed 2022–12–20).

(47) Ryberg, M. W.; Owsianiak, M.; Richardson, K.; Hauschild, M. Z. Development of a Life-Cycle Impact Assessment Methodology

Linked to the Planetary Boundaries Framework. *Ecol. Indic.* **2018**, *88*, 250–262.

(48) Hanafiah, M. M.; Hendriks, A. J.; Huijbregts, M. A. J. Comparing the Ecological Footprint with the Biodiversity Footprint of Products. *J. Clean. Prod.* **2012**, *37*, 107–114.

(49) Guinée, J. B.; de Koning, A.; Heijungs, R. Life Cycle Assessment-Based Absolute Environmental Sustainability Assessment Is Also Relative. *J. Ind. Ecol.* **2022**, *26* (3), 673–682.

(50) Ryberg, M. W.; Owsianiak, M.; Clavreul, J.; Mueller, C.; Sim, S.; King, H.; Hauschild, M. Z. How to Bring Absolute Sustainability into Decision-Making: An Industry Case Study Using a Planetary Boundary-Based Methodology. *Sci. Total Environ.* **2018**, *634*, 1406–1416.

(51) Ryberg, M. W.; Andersen, M. M.; Owsianiak, M.; Hauschild, M. Z. Downscaling the Planetary Boundaries in Absolute Environmental Sustainability Assessments - A Review. *J. Clean. Prod.* **2020**, *276*, 123287.

(52) Hjalsted, A. W.; Laurent, A.; Andersen, M. M.; Olsen, K. H.; Ryberg, M.; Hauschild, M. Sharing the Safe Operating Space: Exploring Ethical Allocation Principles to Operationalize the Planetary Boundaries and Assess Absolute Sustainability at Individual and Industrial Sector Levels. *J. Ind. Ecol.* **2021**, *25* (1), 6–19.

(53) The World Bank. Gross Value Added at Basic Prices (GVA) (Constant 2015 US\$). <https://data.worldbank.org/indicator/NY.GDP.FCST.KD> (accessed 2022–12–10).

(54) Oxford Economics. The Global Chemical Industry: Catalyzing Growth and Addressing Our World's Sustainability Challenges. 2019. <https://www.oxfordeconomics.com/resource/the-global-chemical-industry-catalyzing-growth-and-addressing-our-world-sustainability-challenges/> (accessed 2022–12–20).

(55) Industry Arc. Hydrogen Market - Industry Analysis, Market Size, Share, Trends, Application Analysis, Growth And Forecast 2021–2026. 2020. <https://www.industryarc.com/Research/Hydrogen-Market-Research-501664> (accessed 2022–12–10).

(56) Onel, O.; Niziolek, A. M.; Floudas, C. A. Optimal Production of Light Olefins from Natural Gas via the Methanol Intermediate. *Ind. Eng. Chem. Res.* **2016**, *55* (11), 3043–3063.

(57) Towler, G. P.; Sinnott, R. K. Capital Cost Estimating. In *Chemical Engineering Design: Principles, Practice, and Economics of Plant and Process Design*, 2nd ed.; Butterworth-Heinemann, 2013; Chapter 7, pp 307–354.

(58) Turconi, R.; Boldrin, A.; Astrup, T. Life Cycle Assessment (LCA) of Electricity Generation Technologies: Overview, Comparability and Limitations. *Renew. Sustain. Energy Rev.* **2013**, *28*, 555–565.

(59) International Energy Agency (IEA). Net Zero by 2050: A Roadmap for the Global Energy Sector. 2021. <https://www.iea.org/events/net-zero-by-2050-a-roadmap-for-the-global-energy-system> (accessed 2022–12–20).

(60) Lebreton, L.; Andrady, A. Future Scenarios of Global Plastic Waste Generation and Disposal. *Palgrave Commun.* **2019**, *5* (1), 1–11.

(61) International Energy Agency (IEA). World Energy Outlook 2019. 2019. <https://www.iea.org/reports/world-energy-outlook-2019> (accessed 2022–12–20).

(62) Eurostat-European Commission. EU Trade since 1988 by HS2,4,6 and CN8. 2022. https://ec.europa.eu/eurostat/databrowser/view/DS-045409__custom_4641268/default/table?lang=en (accessed 2023–01–21).

(63) Diaz-Barriga-Fernandez, A. D.; Santibañez-Aguilar, J. E.; Radwan, N.; Nápoles-Rivera, F.; El-Halwagi, M. M.; Ponce-Ortega, J. M. Strategic Planning for Managing Municipal Solid Wastes with Consideration of Multiple Stakeholders. *ACS Sustain. Chem. Eng.* **2017**, *5* (11), 10744–10762.